Royal jelly from different floral sources possesses distinct wound-healing mechanisms and ingredient profiles

Lin, Y., Zhang, M., Lin , T., Wang, L., Wang, G., Chen, T., & Su, S. (2021). Royal jelly from different floral sources possesses distinct wound-healing mechanisms and ingredient profiles. *Food & Function* . Advance online publication. https://doi.org/10.1039/D1FO00586C

Published in:
Food & Function

Document Version:
Peer reviewed version

Queen's University Belfast - Research Portal:
Link to publication record in Queen's University Belfast Research Portal

Royal jelly from different floral sources possesses distinct wound-healing mechanisms and ingredient profiles

Yan Lin [1, #], Meng Zhang [1, 2, #], Tianxing Lin [1], Luying Wang [1], Guanggao Wang [1, 2], Tianbao Chen [3], Songkun Su [1,*]

[1] *College of Animal Sciences (College of Bee Science), Fujian Agriculture and Forestry University, Fuzhou 350002, China*

[2] *Apicultural Research Institute of Jiangxi Province, Nanchang 330052, China*

[3] *Natural Drug Discovery Group, School of Pharmacy, Queen's University, Belfast BT9 7BL, Northern Ireland, UK*

[#] These authors contributed equally to this work.

[*] To whom correspondence should be addressed. College of Animal Sciences (College of Bee Science), Fujian Agriculture and Forestry University, 15 Shangxiadian Road, Cangshan District, Fuzhou 350002, China. Tel. +86-591-83739448; E-mail address: susongkun@zju.edu.cn (S. Su).

Abstract

In recent years, population aging together with the increased prevalence of diabetes and obesity, are fuelling a surge in the instances of cutaneous non-healing wounds. Royal jelly (RJ) is a traditional remedy for wound repair; however, the subjacent mechanisms and ingredient profiles are still largely unknown. Our previous study found that *Castanea mollissima* Bl. RJ (CmRJ-Zj) possessed superior wound healing-promoting effects on both the *in vivo* and *in vitro* models than *Brassica napus* L. RJ (BnRJ-Zj). This study conducted an in-depth investigation on the wound-repairing mechanisms of CmRJ-Zj and BnRJ-Zj to explain the previously observed phenomenon, and also comprehensively characterized their constituents. It was found that chestnut RJ could enhance cutaneous wound healing by boosting the growth and mobility of keratinocytes, modulating the expression of aquaporin 3 (AQP3), regulating MAPK and calcium pathways, and mediating inflammatory responses. By employing LC-MS/MS-based proteomic and metabolomic techniques, the comprehensive molecules present in CmRJ-Zj and BnRJ-Zj were elucidated, resulting in a clear discrimination from each other. A total of 15 and 631 differential proteins and compounds were identified, and 217 proteins were new-found in RJ proteome. With bioinformatic functional analysis, we speculated that some differential components were responsible for the wound-healing properties of CmRJ-Zj. Therefore, this study provides an insight into the wound-healing mechanisms of RJ and is the first to explore the compositions of RJ from different nectar plants. It will facilitate the development of therapeutic agents from RJ to treat difficult-to-heal wounds and the distinction of different RJ categories.

Keywords: royal jelly, wound healing, proliferation, migration, anti-inflammation, aquaporins, proteomics, metabolomics

1 Introduction

As the first line of the body's defence system, skin is essential for maintaining the physiological homeostasis of the human body. Usually, skin has a strong ability to repair naturally. However, owing to the aging of population and the widespread prevalence of diabetes and obesity in recent years, chronic wounds have become a tremendous challenge for healthcare systems around the world [1]. 'Chronic wounds' basically refers to the pathological state of failing to produce anatomically and functionally integrated skin tissue through an orderly and timely repair process within three months [2]. Take the United States for example, about 15% of the elderly suffer from non-healing wounds, including venous stasis ulcers, bedsores, diabetic foot ulcers and even amputation, costing as much as $25 billion annually and severely affecting the quality of patients' lives [3]. Unfortunately, the continued lack of clinically effective and safe drugs for treating problematic wounds, exacerbates the situation. The proportion of the population with chronic wounds is predicted to reach 1-2% in developed countries in the future [2]. Hence, it is of clinical urgency to search for components promoting wound healing functions and to elucidate the mechanisms of action.

Apitherapy, an alternative remedy for illnesses, using bee products such as honey, royal jelly (RJ), propolis, pollen and venom [4], has triggered extensive interest in modern society. Among these natural products, RJ is regarded as a kind of nutritional and valuable food [5], possessing a multitude of biological properties, including antibacterial, anti-inflammatory, immunomodulatory, antioxidant, neuroprotective, and anticancer activities [6–11]. It has been used as a supplement for the treatment of diabetes, cardiovascular disease, Alzheimer's disease, cancer, as well as skin lesions [6,12]. Having used for skin injuries since ancient times [13–16], RJ is proved to be beneficial to the healing of various cutaneous wounds such as diabetic foot ulcers and infected/uninfected wounds in recent years [13,15–17]. Nevertheless, very few studies have focused on its active ingredients and mechanisms of action, greatly limiting the utilisation of RJ and the development of medical agents for treating wounds.

The limited research on RJ may be attributed to the complex compositions, which are difficult to analyse and vary with the differences in floral sources, regions, environmental conditions and honeybee species [18]. The floral sources of RJ depend on the blossom seasons of specific nectariferous plants, during which massive quantities of RJ are produced [19]. It determines the compositions and functions of RJ to a great extent; however, most previous studies ignored this influencing factor when investigating the pharmacological effects of RJ. Studies only compared the proteins in the RJ produced by *Apis mellifera* and *Apis cerana cerana* [5,20], volatile organic components present in RJ from diverse botanical sources [19,21], and antimicrobial activities of RJ from distinct regions [22,23].

Our previous study found that RJ collected during the flowering season of *Vitex negundo* L. (chaste tree) promoted the closure of the *in vitro* wound model of keratinocytes, and it was speculated that some major royal jelly proteins (MRJPs) might be responsible for such activity [24]. And we also preliminarily realised that chestnut RJ/their extracts were beneficial to the healing of the *in vivo* wound model and to the cellular proliferation and migration, while rapeseed RJ and their extracts were devoid of those effects; the extracts from both kinds of RJ displayed different degrees of anti-inflammatory activities [17]. Nonetheless, the exact compositions underlying the different RJ, the precise mechanisms of action, and the corelation between the constituents and the functions, are almost unrevealed. Therefore, here we carried out an in-depth exploration of the wound-healing mechanisms of the effective crude RJ, and were the first to thoroughly analyse the constituent profiles of chestnut and rapeseed RJ via LC-MS/MS-based proteomic and metabolomic techniques. In the meantime, we analysed the relationship between the effectiveness and the differential components. It will lay the foundation for future studies to facilitate the application of specific RJ for the treatment of difficult-to-heal wounds, and provide clues towards the development of wound care agents as well as the identification of different kinds of RJ.

2 Materials and methods

2.1 RJ samples harvesting and preparation

RJ samples, produced by western honeybees (*Apis mellifera* L.), were harvested in different regions of P.R. China as previously described [17]. Details about RJ samples are listed in Table 1. Nectar plants were validated taxonomically by Yan Lin using the Kew Medicinal Plant Names Services (MPNS). The voucher specimens were deposited in the herbarium of our institute, with deposition numbers of CmZj-20180601, CmHb-20190601, BnZj-20190401, BnHb-20180401, and BnJs-20190401. This study was approved by the Fujian Agriculture and Forestry University Ethical Review Board (No. PZCASFAFU2019008). In subsequent bioassays, RJ samples were initially prepared as stock solutions at 2,000 or 8,000 μg/ml that were double-diluted in serum-free medium to obtain a series of working solutions.

Table 1: Details of RJ samples collected during the blossom seasons of diverse nectariferous plants in different geographical origins

Royal jelly	Nectariferous plants	Geographical regions	Florescence
CmRJ-Zj	*C. mollissima* Bl.	Zhejiang Province/29 °50'N, 150 °90'E	June 2018
CmRJ-Hb	*C. mollissima* Bl.	Hebei Province/39 °57'N, 118 °60'E	June 2019
BnRJ-Zj	*B. napus* L.	Zhejiang Province/29 °50'N, 150 °90'E	April 2019
BnRJ-Hb	*B. napus* L.	Hubei Province/31 °10'N, 112 °34'E	April 2018
BnRJ-Js	*B. napus* L.	Jiangsu Province/32 °34'N, 119 °27'E	April 2019

2.2 Cell culture and cell viability assay

The immortalized human epidermal keratinocytes (HaCaT cells, DSMZ No. 771), human embryonic skin fibroblasts (CCC-ESF-1 cells, HS-C1083), and murine macrophages (RAW 264.7 cells, No. TCM13) were cultured as previously described [17].

The proliferative effects of RJ samples on keratinocytes were evaluated with MTT assay as previously described [17]. Briefly, HaCaT cell suspension (3.5×10^3 cells/well) was cultivated for 24 h. Before exposure to RJ samples at a range of concentrations (3.90-2,000 μg/ml) for 48 h, cells were subjected to starvation for 12 h in serum-free medium. Absorbance was measured at 492 nm after 4-h incubation in MTT (Beyotime, Shanghai, China) and dissolution of formazan crystals in DMSO. Cell viability refers to the absorbance of RJ treated cells relative to that of vehicle treated cells (control).

Cytotoxicity of RJ samples towards human dermal fibroblasts was also evaluated with MTT assay as described above using CCC-ESF-1 cells.

CCK-8 colorimetric assay was conducted to examine the cytotoxicity of RJ samples towards macrophages. It resembled the MTT assay; however, the density of RAW 264.7 cell suspension seeded was 1.0×10^7 cells/ml and the cells were exposed to RJ for 24 h before the addition of Cell Counting Kit-8 solution (CCK-8, 5%, 10 μl, Transgen, Beijing, China). The samples were tested at concentrations between 15.63 and 8,000 μg/ml, and the absorbance was measured directly at 450 nm without removing the supernatants.

2.3 Scratch wound assay

The effect of RJ on the mobility of keratinocytes was assessed by the *in vitro* scratch wound assay as previously described [17]. Briefly, confluent HaCaT cells (3.5×10^4 cells/well) with a gap in the middle of cell monolayers were treated with RJ (7.81 to 31.25 μg/ml) or medium alone (control) for 24 h. Re-epithelialization rates were calculated as percentages of changes in wound areas between 0 h and 12/24 h with respect to the initial wound areas.

In order to investigate the mechanisms of action of RJ on wound closure, some well-characterized inhibitors, interfering with the signalling pathways of cell migration, were added in combination with RJ samples, followed by incubation for 24 h. More specifically, extracellular signal regulated kinase (ERK) inhibitor (PD98059, 10 μM, MCE, New Jersey, USA), p38 inhibitor (SB203580, 15 μM, MCE, New Jersey, USA), and cell-permeant calcium chelator (BAPTA-AM, 5 μM, MCE, New Jersey, USA) were applied.

2.4 Cell migration assay

Transwell cell migration assay was conducted to evaluate the chemoattractant activities of RJ towards HaCaT cells. A total of 8×10^4 cells suspended in serum-free medium were seeded into the upper

compartments of transwell plates (8-μm pore size, Millipore, Massachusetts, USA), while the lower compartments were filled with 2 ml of serum-free medium in the presence or absence of RJ (15.63-62.50 μg/ml). Cells were allowed to grow and migrate for 24 h. The upper compartments were then washed twice with PBS, followed by fixation with 800 μl of paraformaldehyde (4%) for 15 min and subsequent staining with 0.1% crystal violet for a further 15 min. Then, the compartments were washed again with PBS to remove extra crystal violet and the non-migratory cells in the upper filter side were swept away with a cotton swab. The filter with migrated cells was observed with an inverted microscope (Olympus, Tokyo, Japan). The dye was dissolved in 200 μl of 33% acetic acid and the absorbance was measured at 570 nm using a microplate reader (Infinite F50, Tecan, Männedorf, Austria). Cell migration rate (%) represented the absorbance of migrated cells treated with RJ relative to those treated with serum-free medium $\times 100\%$.

2.5 Cytosolic calcium measurement

Cytosolic free Ca^{2+} was measured using a Fluo-4 NW Calcium Assay Kit (Invitrogen, Paisley, UK) according to the manufacturer's instruction with minor modifications. Briefly, HaCaT cells (3.5×10^4 cells/well) were seeded to 96-well plates and grown for 24 h. Washed with PBS, cells were then incubated with 100 μl of dye loading buffer composed of 2.5 mM probenecid, 20 mM HEPES (Solarbio, Shanghai, China) and Fluo-4 NW dye mix (supplied by the kit) in 10 ml of D-Hanks' balanced salt solution (Coolaber, Beijing, China) with or without $CaCl_2$ (2 mM) for 45 min at 37 ℃. The variation of cytosolic free Ca^{2+} was monitored by measuring the fluorescent intensity at 1-min interval, 37 ℃, with excitation and emission wavelength of 494 and 516 nm over 60 min in a Varioskan^{TM} LUX microplate reader (Thermo Scientific, Waltham, MA, USA).

2.6 Quantitative real-time PCR

To quantify the transcriptional expression of aquaporins, quantitative real-time PCR was implemented. HaCaT cells (1.6×10^5 cells/well) were placed into 6-well plates and grown for 24 h.

After starvation for 12 h using serum-free medium, cells were treated or not treated with various concentrations of RJ samples (7.81-125 μg/ml) for 24 h. Trizol Reagent (TransGen, Beijing, China) was applied in the extraction of total RNA, followed by concentration and purity confirmation with a NanoDrop 2000 Spectrophotometer (Thermo Scientific, Waltham, MA, USA). The resultant RNA was then subjected to elimination of genomic DNA with gDNA wiper Mix (Vazyme, Nanjing, China) and reverse transcription for cDNA synthesis with HiScript III RT SuperMix for the subsequent qPCR (Vazyme, Nanjing, China) following the manufacturer's instruction. Real-time PCR was executed with ChamQTM SYBR Color qPCR Master Mix (Vazyme, Nanjing, China) and specific primers for AQP1, AQP3, AQP5 and glyceraldehyde-3-phosphate dehydrogenase (GAPDH) as listed in Table 2. The relative mRNA expression levels of target genes were normalized to GAPDH gene expression levels.

Table 2: Primers used for quantitative real-time PCR

Genes	Forward (5'-3')	Reverse (5'-3')
AQP1	CTGGGCATCGAGATCATCGG	ATCCCACAGCCAGTGTAGTCA
AQP3	GGGGAGATGCTCCACATCC	AAAGGCCAGGTTGATGGTGAG
AQP5	CGGGCTTTCTTCTACGTGG	GCTGGAAGGTCAGAATCAGCTC
GAPDH	GGAGCGAGATCCCTCCAAAA	GGCTGTTGTCATACTTCTCATGG

2.7 Western blotting analysis

To analyse the AQP3 protein expression level, 1.6×10^5 HaCaT cells were cultured in each well of 6-well plates for 24 h. They were then exposed to a series of RJ (7.81-125 μg/ml) or vehicle alone for 24 h after 12-h starvation in serum-free medium, followed by washing twice with icy PBS and cytolysis with lysis buffer (Beyotime, Beijing, China). Cell lysate was centrifuged (4 ℃, 8,600 ×g, 10 min) to obtain the supernatant containing total proteins, the concentration of which was measured by BCA protein assay kit (TransGen, Beijing, China). SDS-PAGE (12%) was used to separate proteins which were then transferred onto polyvinylidene fluoride (PVDF) membranes. Blots were probed with primary antibodies against AQP3 (1:1,000, Sigma-Aldrich, Saint Louis, USA), β-2-

microglobulin (B2M, 1:10,000, Abcam, Cambridge, USA) and GAPDH (1:2,000, TransGen, Beijing, China) overnight at 4℃, and incubation with secondary antibody (1:10,000, Abcam, Cambridge, USA) for 1 h at room temperature was followed. Immunoblots were subsequently developed with enhanced chemiluminescence (ECL, Bio-Rad, Hercules, USA) reaction. AQP3 protein expression level was expressed as AQP3/B2M or AQP3/GAPDH densitometric ratio.

To analyse the activation of p38 and ERK1/2, HaCaT cells were subjected to scratch wound assay in the presence or absence of CmRJ-Zj (15.63 μg/ml) for 0, 0.25, 0.5, 1, 6, 12 and 24 h. Blots were probed with primary antibodies against p38, p-p38, ERK1/2 (1:1,500, ABclonal, Wuhan, China), p-ERK1/2 (1:1,000, Abclonal, Wuhan, China) and GAPDH overnight at 4℃, and incubation with secondary antibody for 1 h at room temperature was followed. Phosphorylation of p38 and ERK1/2 was expressed as p-p38/p38 and p-ERK1/2 / ERK1/2 densitometric ratio, respectively.

2.8 RNA interference (RNAi)

To establish keratinocytes with AQP3 knockout, three specific small interfering RNAs (siRNAs) and a general non-targeting siRNA (siN) [25,26] were synthesised by GenePharma (Shanghai, China) (Table 3). A total of 6 $\times 10^5$ HaCaT cells were cultured in each well of 6-well plates overnight to reach ~80% confluence. GP-transfect-Mate (16 μl, GenePharma, Shanghai, China) and siRNA (20 μl, 20 μM) were separately diluted in 200 μl of Opti-MEM (Gibco, Thermo Fisher Scientific, New York, USA) and then incubated at room temperature for 5 min. They were mixed thoroughly and incubated at room temperature for a further 20 min to form the transfection complex. It was followed by adding the complex to each well containing 1.6 ml of Opti-MEM. The inhibition of each siRNA on the expression of AQP3 was analysed by qRT-PCR for mRNA and western blotting for protein. Cells were trypsinised and collected for the subsequent cell viability and scratch wound assays.

Table 3: siRNAs for RNA interference

siRNA	Forward (5'-3')	Reverse (5'-3')

siAQP3-159	GUGGUUUCCUCACCAUCAATT	UUGAUGGUGAGGAAACCACTT
siAQP3-360	GGCUGUAUUAUGAUGCAAUTT	AUUGCAUCAUAAUACAGCCTT
siAQP3-450	CCUCUGGACACUUGGAUAUTT	AUAUCCAAGUGUCCAGAGGTT
siN	GCGACGAUCUGCCUAAGAU	AUCUUAGGCAGAUCGUCGC

2.9 Evaluation of inhibitory activity on NO production

The amount of NO produced by macrophages after treatment of RJ samples was estimated as previously described [17]. Briefly, RAW 264.7 cells (5.0×10^6 cells/well) were incubated with serum-free medium in the presence or absence of RJ (125 and 1000 μg/ml), followed by addition of LPS from *Escherichia coli* (1 μg/ml, Sigma-Aldrich, Saint Louis, USA) and further incubation for 24 h. Culture supernatants were reacted with Griess reagent and NO production was expressed as % of LPS = OD value of RJ and LPS treated cells / OD value of LPS treated cells × 100%.

2.10 Enzyme-linked immunosorbent assay (ELISA)

The anti-inflammatory effects of RJ on the secretion of tumour necrosis factor-α (TNF-α) and transforming growth factor-β1 (TGF-β1) in macrophages were evaluated employing ELISA as previously described [17]. In brief, cell supernatants collected above were used to determine the levels of cytokines using ELISA kits (Dakewe, Beijing, China).

2.11 Proteomic analysis of RJ from different floral sources

Proteins in RJ were identified and quantified by Label-free protein quantification method. Samples (CmRJ-Zj and BnRJ-Zj, 100 mg) were homogenized in 1 ml of lysis buffer (100 mM NH_4HCO_3, 6 M Urea, 0.2% SDS, pH = 8). After centrifugation, the supernatant was reacted with 2 mM dithiothreitol (DTT) for 60 min at 56 ℃ and sufficient iodoacetamide for 1 h. Proteins were washed and precipitated with pre-cooling acetone at -20 ℃ for 2 h. Following centrifugation, precipitation was dissolved in dissolution buffer composed of 6 M urea and 0.1 M triethylammonium bicarbonate

(pH = 8.5). The concentration of RJ total proteins was determined using Bradford protein assay kit (Bio-Rad, Hercules, USA), followed by electrophoretic analysis with 12% SDS-PAGE gels.

The resulting total proteins (20 μg) dissolved in dissolution buffer were digested with Trypsin Gold (Promega, Madison, USA) overnight at 37 ℃. Peptide mixture was desalted using ZipTip C18 pipette tips (Millipore, Bedford, MA, USA).

Proteomic analysis was implemented employing an EASY-nLC^{TM} 1200 UHPLC system (Thermo Fisher, Waltham, MA, USA) equipped with a home-made pre-column (C18 Nano-Trap column, 2 cm × 75 μm, 3-μm particle) and an analytical column (C18, 15 cm × 150 μm, 1.9-μm particle), coupled with an Orbitrap Q Exactive HF-X mass spectrometer (Thermo Fisher, Waltham, MA, USA) with a nano electrospray ionization (NSI) source. Peptides were eluted with eluent A (formic acid/ACN/water, 0.1/2.0/97.9, v/v/v) and eluent B (formic acid/acetonitrile (ACN)/water, 0.1/90.0/9.9, v/v/v) over 90 min at a flow rate of 500 nl/min with the gradient programme of 0-62 min, 4%-23% B; 62-82 min, 23%-35% B; 82-86 min, 35%-80% B; 86-90 min, 80% B. Mass spectrometric analysis was operated in positive ion mode with capillary temperature and spray voltage of 320 ℃ and 2.2 kV, respectively. The 40 most abundant precursor ions from full MS scan (400-1500 m/z) were fragmented by higher energy collisional dissociation (HCD) and further analysed with an automatic gain control (AGC) target value of 5×10^4, a maximum ion injection time of 40 ms, an intensity threshold of 2.5×10^5 ions/s, and the dynamic exclusion parameter of 30 s. Finally, the resulting spectra were analysed using the Maxquant (version 1.6.15.0, Max Planck Institute of Biochemistry, München, Germany) against the NCBI database (*Apis mellifera*, *Castanea mollissima*, *Brassica napus*, and *Citrullus lanatus*). Protein contents and their potential functions were determined and predicted as described previously [24].

2.12 Metabolomic analysis of RJ from different floral sources

The small molecules (<1,000 Da) present in RJ samples (CmRJ-Zj and BnRJ-Zj) were further analysed employing LC-MS/MS technology. RJ (100 mg) was ground in liquid nitrogen, dissolved in 500 μl of 80% methanol (containing 0.1% formic acid) and kept on ice for 5 min. After centrifugation, the methanol in the supernatant was diluted to 60%, and it was filtered with 0.22-μm membrane for the subsequent analysis. The resultant sample was subjected to liquid chromatographic analysis using an LC20 UHPLC (Shimadzu, Kyoto, Japan) fitted with a Waters ACQUITY UPLC HSS T3 C18 column (100 × 2.1 mm, 1.8-μm particle, Waters, MA, USA). Elution was fulfilled at a flow rate of 0.4 ml/min with eluent A (0.1% formic acid in water) and eluent B (0.1% formic acid in CAN) using a gradient program: 0-11 min, 5%-90% B; 11-12 min, 90% B; 12-12.1 min, 90%-5% B; 12.1-14 min, 5% B. Mass spectrometric analysis was performed in both positive and negative ion modes employing a Triple TOF-6600 mass spectrometer (AB Sciex, MA, USA). In ESI source, capillary temperature and spray voltage were maintained at 550 ℃ and 5.0 kV, respectively. The MS raw data was converted into mzML format with ProteoWizard software, followed by peak extraction, alignment and retention time correction in XCMS program. Peaks were filtered by deletion rate > 50%. Molecules with m/z 100-1500 were identified by searching against mzCloud and Chemspider databases. The processed data were subjected to univariate analysis and multivariate analysis.

2.13 Statistical Analysis

All data was analysed using GraphPad Prism 5.0 software (CA, USA). Significance of differences was calculated by the one-way ANOVA method followed by Tukey's test, and differences with $p<0.05$ were considered as statistically significant. All values were presented as mean values ± standard errors (SEM).

3 Results

3.1 Effects of RJ on the proliferation of keratinocytes

As the propagation of keratinocytes is essential for wound healing, especially in the proliferation stage [27], RJ samples derived from different nectar plants, regions, and years of acquisition, were examined preliminarily for their proliferative effects on human epidermal keratinocytes (HaCaT). As shown in Figure 1, among the tested RJ samples, those collected in the blossom season of *C. mollissima* Bl., regardless of the geographical origins or the sampling years, promoted the growth of HaCaT cells at the concentrations of 3.90-250 μg/ml. Conversely, none of the RJ collected in the flowering season of *B. napus* L. exhibited growth-promoting effects on the cells, and even caused severe cytotoxicity at some lower concentrations. The data implied that the botanical sources might be the determinant factor influencing the bioactivity of RJ. Notably, *C. mollissima* Bl. RJ could also have negative impacts on the cell viability at high doses (>1,000 μg/ml) (Figure 1A and B). Thus, RJ samples at lower concentrations were applied in further investigations of their potential wound healing activities.

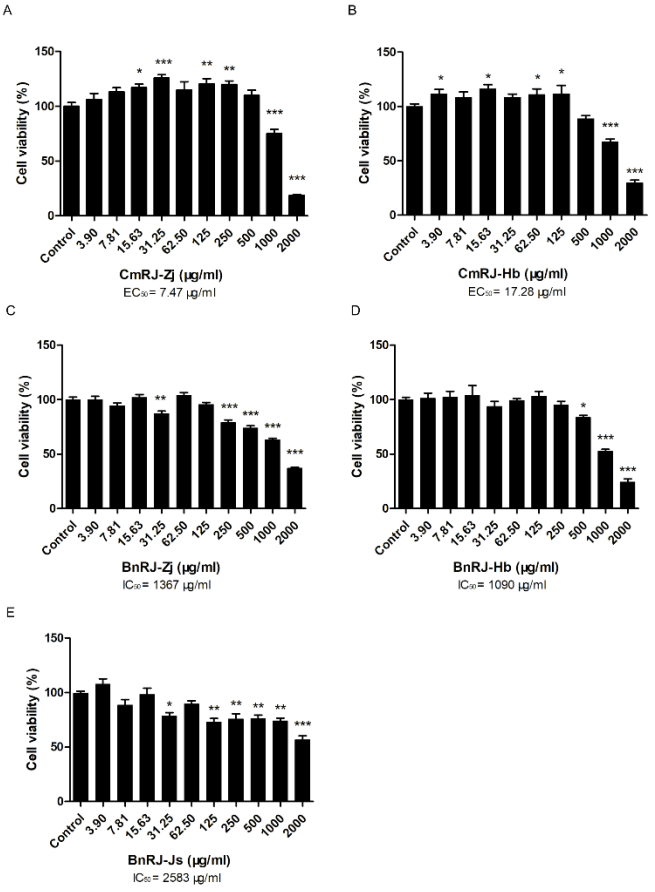

Figure 1: Proliferative effects of RJ from different floral sources and regions on HaCaT cells after treatment for 48 h. Effects of chestnut RJ from Zhejiang (CmRJ-Zj) and Hebei (CmRJ-Hb) Provinces **(A-B)** and rapeseed RJ from Zhejiang (BnRJ-Zj), Hubei (BnRJ-Hb) and Jiangsu (BnRJ-Js) Provinces **(C-E)** on the growth of HaCaT cells. *, $p < 0.05$; **, $p < 0.01$; ***, $p < 0.001$, compared with control.

3.2 Effects of RJ on the migration of keratinocytes

Re-epithelialization involving the migration of keratinocytes is important for the completion of wound closure in the wound healing process [27]. Accordingly, it is worth investigating the migratory potency of RJ towards HaCaT cells. As the biological activities of RJ seemed to be mainly dependent on the floral origins, CmRJ-Zj possessing the most potent proliferative efficacy in MTT assay and BnRJ-Zj from the same apiaries were selected for further study.

To observe their migratory effects on keratinocytes, an *in vitro* scratch wound assay of HaCaT monolayer cells was initially performed. Obviously, as time went on, many more cells treated with CmRJ-Zj moved from both sides of the scratch wounds towards the centre compared with untreated cells. The cells, treated with 7.81 μg/ml of CmRJ-Zj for 24 h, exhibited the best performance. The wound closure rate increased to 69.58% (Figure 2A). In contrast, there was no prominent difference in the mobility of cells exposed to BnRJ-Zj and medium (Figure 2B). It suggested that chestnut RJ might have the ability to promote the migration of keratinocytes, accelerating wound repair, while rapeseed RJ appeared to produce no such effect.

Since CmRJ-Zj also possessed cell growth-promoting effects at 48 h (Figure 1A), to eliminate the potential interference, and provide evidence of whether it had direct effects on the cytotaxis, a chemotaxis assay was conducted using transwell plates. As shown in the micrographs in Figure 2C and D, when treated with CmRJ-Zj, a substantial quantity of cells migrated to the lower chamber side of the filter compared with the control, while no obvious difference was observed between the cells

exposed to BnRJ-Zj and medium. With quantification by measuring the absorbance, it further proved that the migration of HaCaT cells treated with CmRJ-Zj increased significantly by about 35% relative to control (Figure 2C), while the cells incubated with BnRJ-Zj did not display any marked tendency (Figure 2D). It suggested that CmRJ-Zj had a direct chemoattractant effect on keratinocytes.

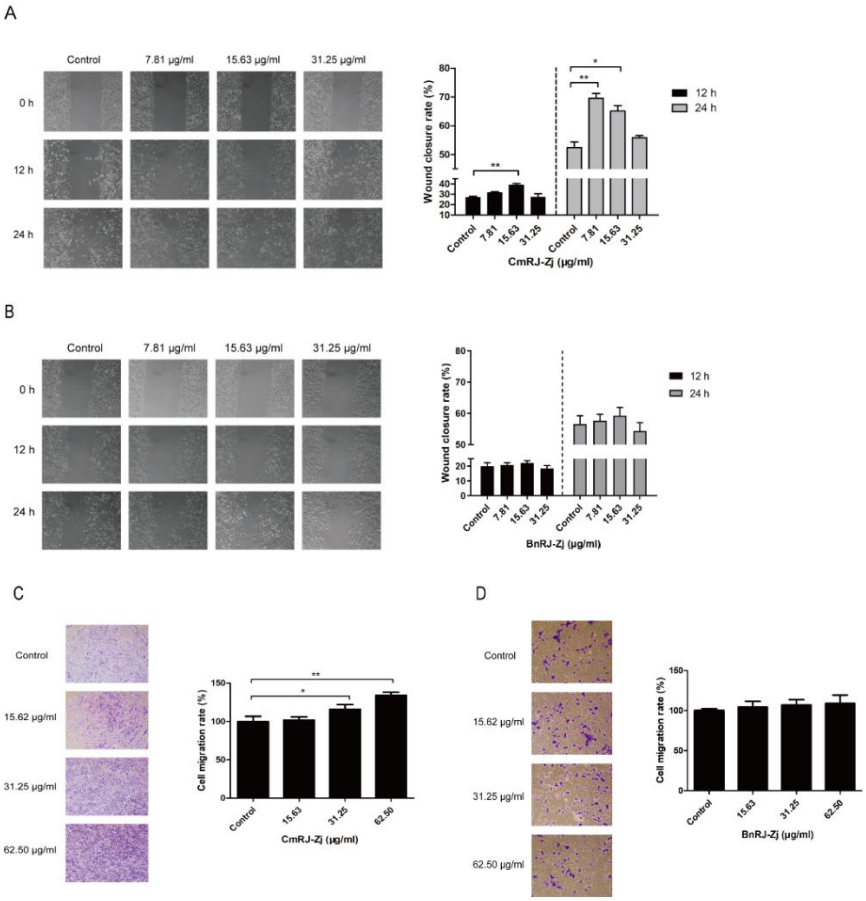

Figure 2: Migratory effects of RJ from different floral sources on HaCaT cells. (A-B) Migration of HaCaT cells treated with CmRJ-Zj and BnRJ-Zj, respectively. Left panels, observation of the migratory manners of HaCaT cells at 12 and 24 h post-scarification. Right panels, wound closure rates of HaCaT cells. **(C-D)** Chemoattractant effects of CmRJ-Zj and BnRJ-Zj on HaCaT cells, respectively. Left panels, micrographs of migrated cells on the transwell filter. Right panels, migration rates of HaCaT cells. *, $p < 0.05$; **, $p < 0.01$.

3.3 Effects of RJ on the MAPK and Ca^{2+} signalling pathways

In order to explore the modulation of CmRJ-Zj on MAPK pathway, the scratch wounds of HaCaT monolayers treated with or without it (15.63 μg/ml) were investigated for the activation of p38 and ERK1/2 by western blotting. Compared with the basal level (0 h), without RJ treatment, scratch wounding significantly induced the phosphorylation of p38 by 3-fold within 1 h, but not of ERK1/2; however, exposure to CmRJ-Zj facilitated remarkably higher and prompter phosphorylation of p38 and ERK1/2 than the corresponding untreated groups within 6 h. The activation of p38 and ERK1/2 reached the highest level at 1 h and 15 min post-wounding, respectively, with the treatment of CmRJ-Zj (Figure 3A). In addition, in the presence of extracellular Ca^{2+}, CmRJ-Zj time-dependently elevated the intracellular Ca^{2+} relative to the RJ-untreated cells in a significant way (Figure 3B-C). When the scratch wounds were treated with ERK inhibitor (PD98059), p38 inhibitor (SB203580), and cell-permeant calcium chelator (BAPTA-AM), CmRJ-Zj-mediated cell migration was completely abolished (Figure 3D). These results collectively indicated that activation of p38, ERK1/2, and calcium signalling pathways was essential for the CmRJ-Zj-modulated wound closure.

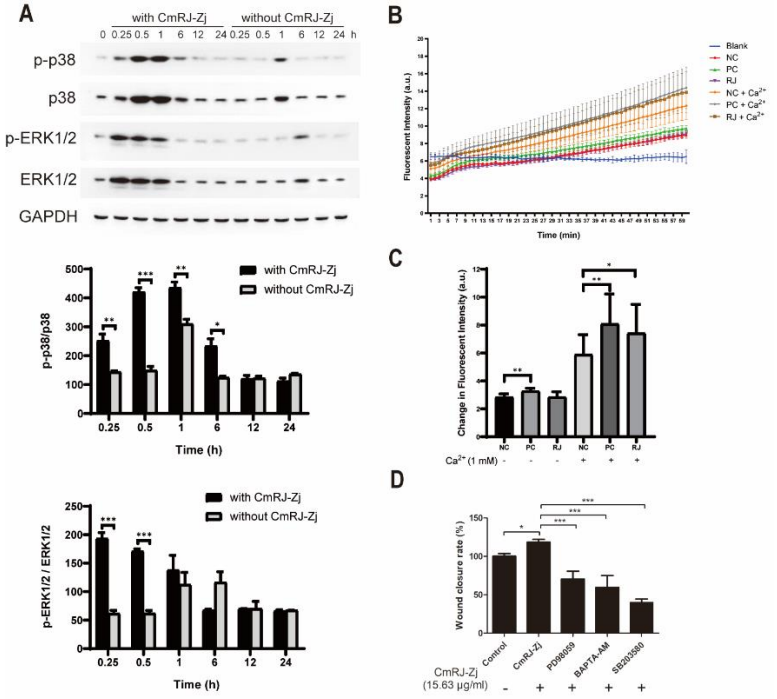

Figure 3: Effects of CmRJ-Zj on MAPK and Ca^{2+} signalling pathways. (A) Western blots displaying the expression of p-p38, p38, p-ERK1/2 and ERK1/2. The ratios of the phosphorylated

forms to the total proteins were normalized to the basal level (0 h). GAPDH acted as an internal control. **(B)** Track of changes in the cytosolic free Ca^{2+} detected with Fluo-4 NW kit at 1-min interval over 60 min. **(C)** Changes in the cytosolic free Ca^{2+} between 0 and 60 min. NC, PC and RJ represents cells treated with vehicle alone, calcium ionophore A23187 (500 μM, Aladdin, Shanghai, China) and CmRJ-Zj (15.63 μg/ml), respectively. **(D)** Effects of different signalling pathway inhibitors on CmRJ-Zj-induced wound closure of HaCaT monolayers. *, $p < 0.05$; **, $p < 0.01$; ***, $p < 0.001$.

3.4 Modulatory effects of RJ on aquaporins (AQPs) expression

Aquaporins, transmembrane proteins responsible for the transport of water and glycerol, are critical for skin hydration and wound healing [28–30]; hence, the expression of these proteins in keratinocytes induced by CmRJ-Zj and BnRJ-Zj was measured by quantitative real-time PCR and western blotting. In the qRT-PCR analysis, AQP1, AQP3 and AQP5 mRNA expressions were determined, in which only CmRJ-Zj at the concentration of 15.63 μg/ml significantly elevated the mRNA level of AQP3 in HaCaT cells (Figure 4B), while it dramatically decreased the mRNA level of AQP1 at 125.00 μg/ml (Figure 4A) and BnRJ-Zj greatly reduced AQP5 mRNA level at some concentrations (7.81 and 31.25 μg/ml) (Figure 4C). Thus, it seemed that neither CmRJ-Zj nor BnRJ-Zj could stimulate the mRNA expression of AQP1 or AQP5 at tested concentrations. Interestingly, the protein expression level of AQP3 in HaCaT cells exposed to CmRJ-Zj was totally different from the mRNA expression pattern. At the effective concentration (15.63 μg/ml) in qRT-PCR assay, CmRJ-Zj did not exhibit any modulatory effect on the AQP3 protein expression; however, the level of AQP3 protein was extremely down-regulated by 62.50 μg/ml of CmRJ-Zj, while exceedingly up-regulated at 125.00 μg/ml with respect to control (Figure 4D).

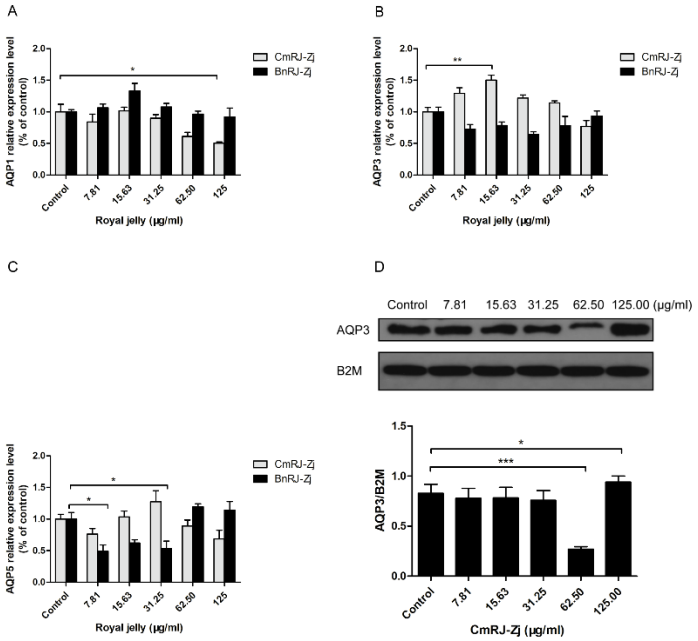

Figure 4: Effects of RJ from different floral sources on the expression of aquaporins (AQPs) in human keratinocytes. (A-C) Expression of AQP1, AQP3 and AQP5 mRNAs in HaCaT cells after treatment of CmRJ-Zj or BnRJ-Zj for 24 h. GAPDH acted as an internal control. **(D)** Expression of AQP3 protein in HaCaT cells after exposure to CmRJ-Zj for 24 h. B2M acted as an internal control. *, $p < 0.05$; **, $p < 0.01$; ***, $p < 0.001$.

3.5 Effects of AQP3 knockdown on RJ-mediated HaCaT proliferation and migration

To investigate the role of AQP3 in the CmRJ-Zj-induced cell behaviour, RNAi was carried out to establish AQP3 silenced keratinocytes. Compared with control, non-targeting siRNA (siN) influenced neither the mRNA nor the protein expression level of AQP3, whereas siAQP3-159 showed the strongest inhibitory effect on the expression of both AQP3 mRNA and protein by 90% and 80%, respectively (Figure 5A-B). It suggested that siN did not interfere with the expression of AQP3, and the interference caused by siAQP3-159 was the most effective; hence, they were suitable to be selected for the subsequent cell viability and scratch wound assays.

In cell viability assay, CmRJ-Zj-induced proliferation was maintained in siN-transfected HaCaT cells, while the effect was completely supressed after silencing of AQP3 (Figure 5C). Similarly, in siN

group, CmRJ-Zj significantly accelerated the wound closure of keratinocytes, while siRNA-mediated AQP3 suppression led to the restraint of CmRJ-Zj-induced cell migration at both 12 and 24 h post-wounding (Figure 5D). These results revealed that AQP3 played a vital role in the *in vitro* wound healing mediated by CmRJ-Zj.

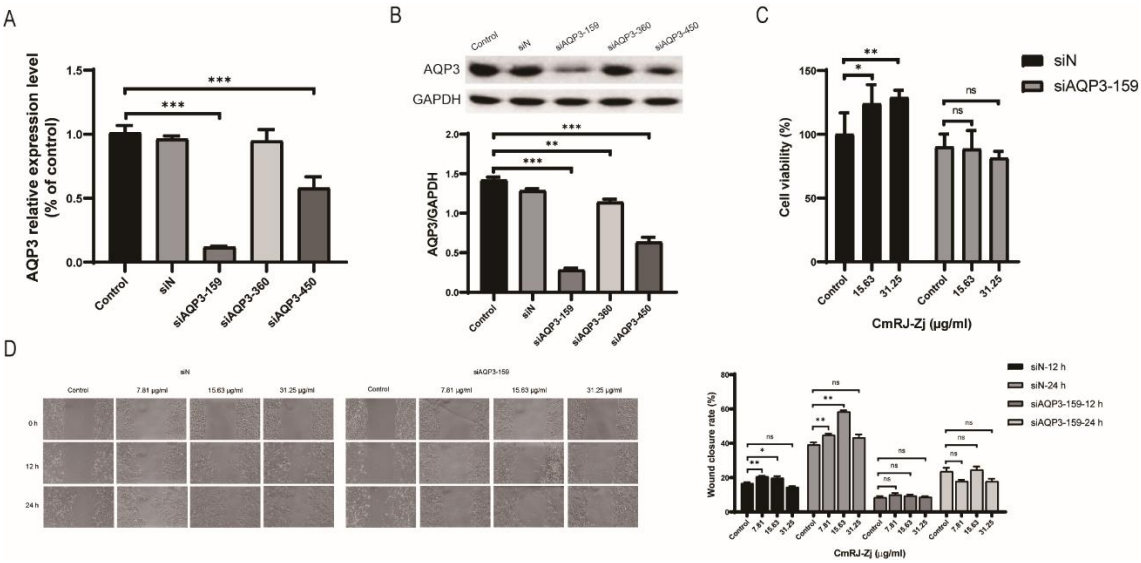

Figure 5: AQP3 knockdown and the effects on the CmRJ-Zj-induced cell proliferation and migration. (A) AQP3 mRNA expression analysed by qRT-PCR after RNAi. **(B)** AQP3 protein expression analysed by western blotting after RNAi. GAPDH acted as an internal control. Control, cells without siRNA transfection. Effects of CmRJ-Zj on HaCaT proliferation and migration following AQP3 knockdown as assessed by cell viability assay **(C)** and scratch wound assay **(D)**. Control, cells treated with vehicle alone. *, $p < 0.05$; **, $p < 0.01$; ***, $p < 0.001$.

3.6 Anti-inflammatory effects of RJ on macrophages

The pro-inflammatory stimuli LPS-induced macrophages (RAW 264.7), which would produce a host of NO and cytokines such as TNF-α and TGF-β1, were used to assess the anti-inflammatory potency of RJ. The dose of LPS (1 μg/ml) used for stimulating inflammation was based on previous studies [31,32]. RJ samples (CmRJ-Zj and BnRJ-Zj) were examined for their cytotoxicity towards macrophages in the first place, and were found to be devoid of toxicity below the concentration of 1,000 μg/ml

(Figure 6A and B). Thus, concentrations lower than that were applied in the subsequent *in vitro* anti-inflammatory assays. As shown in Figure 6C, both kinds of RJ prominently suppressed the LPS-induced NO production in a dose-dependent manner. Nonetheless, apart from 1,000 μg/ml of BnRJ-Zj significantly inhibiting the TNF-α production, CmRJ-Zj did not affect the LPS-stimulated TNF-α level in RAW 264.7 cells (Figure 6D). Inversely, both types of RJ dose-dependently increased the generation of TGF-β1 with statistical significance, in which CmRJ-Zj was more potent than BnRJ-Zj, resulting in a 3-fold increase in TGF-β1 level at the concentration of 1,000 μg/ml compared with only LPS-induced cells (Figure 6E). The results suggested that both RJ samples might be effective against the LPS-stimulated inflammation with different mechanisms.

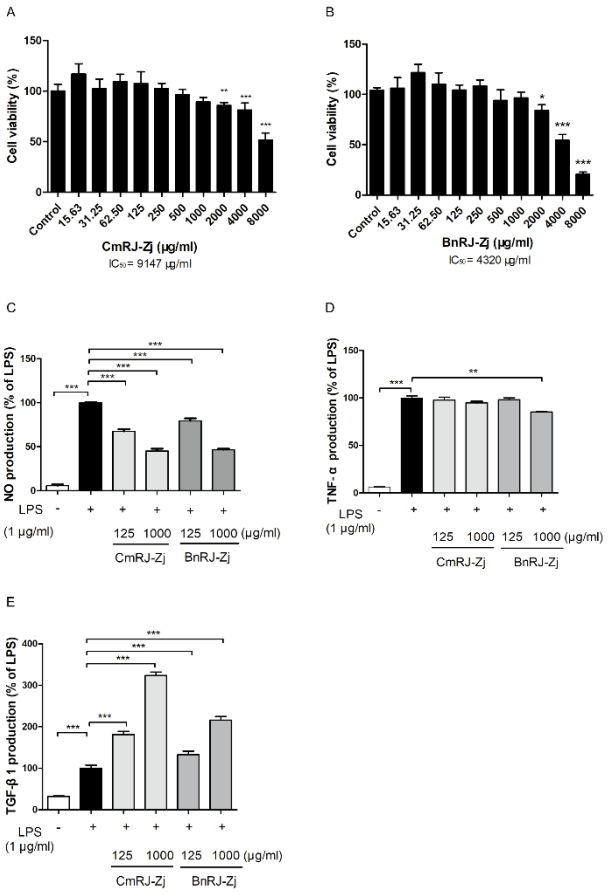

Figure 6: Effects of RJ from different floral sources on LPS-stimulated inflammatory responses. (A-B) Cytotoxic effects of CmRJ-Zj and BnRJ-Zj on RAW 264.7 cells. *, $p < 0.05$; **, $p < 0.01$; ***, $p < 0.001$, compared with control. **(C-E)** Modulatory effects of CmRJ-Zj and BnRJ-Zj

on the production of NO, TNF-α and TGF-β1 in LPS-stimulated microphages. **, $p < 0.01$; ***, $p < 0.001$.

3.7 Cytotoxicity of RJ towards human dermal fibroblasts

Since fibroblasts are also important cells participating in the wound healing process, the cytotoxicity of CmRJ-Zj and BnRJ-Zj towards a human embryonic skin fibroblast cell line (CCC-ESF-1) was examined. As shown in Figure 7A, CmRJ-Zj was devoid of toxicity towards CCC-ESF-1 cells at concentrations below 1,000 μg/ml and could even significantly facilitate cell growth at some concentrations (250-500 μg/ml). On the contrary, BnRJ-Zj could not enhance the growth of CCC-ESF-1 cells and was even toxic at some concentrations (Figure 7B).

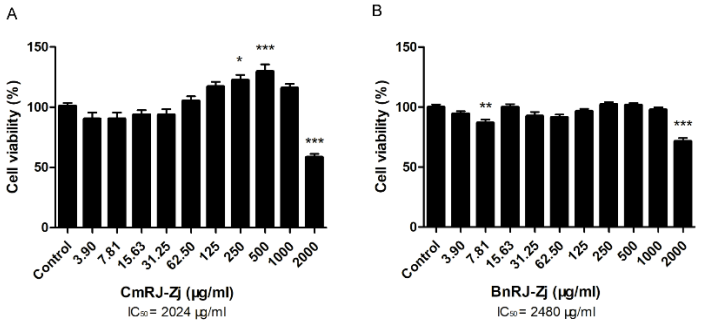

Figure 7: Cytotoxicity of RJ from different floral sources towards CCC-ESF-1 cells after treatment for 48 h. Effects of CmRJ-Zj **(A)** and BnRJ-Zj **(B)** on CCC-ESF-1 cells. *, $p < 0.05$; **, $p < 0.01$; ***, $p < 0.001$, compared with control.

3.8 Identification and quantification of proteins present in RJ

A total of 292,690 spectra, 1,280 peptides and 233 proteins were identified from CmRJ-Zj and BnRJ-Zj, 102 of which were quantifiable proteins. Principle component analysis (PCA) indicated that CmRJ-Zj and BnRJ-Zj were clearly distinguished from each other (Figure 8A). Herein, we identified 15 differentially expressed proteins (DEPs) using a fold change (FC) > 1.5 or < 1/1.5 (p value < 0.05), 7, 3 and 5 proteins being up-regulated, down-regulated and uniquely expressed in CmRJ-Zj vs. BnRJ-

Zj (Figure 8B and Table S1). GO enrichment analysis showed that exopeptidase activity (GO:0008238, 2 DEPs, *p* value < 0.05) was the most enriched GO term. In KEGG analysis, DEGs were mainly involved in starch and sucrose metabolism (mpa00500, 2 DEGs, *p* value < 0.05). The mass spectrometry proteomics data has been deposited to the ProteomeXchange Consortium (http://proteomecentral.proteomexchange.org) via the iProX partner repository [33] with the dataset identifier PXD028228.

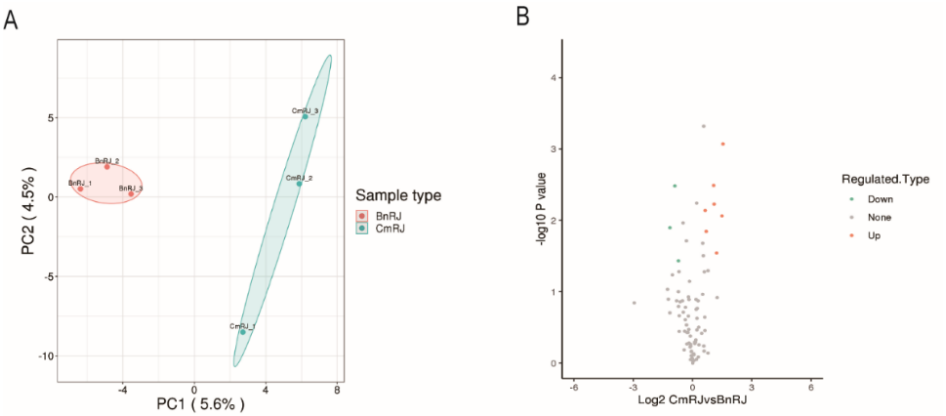

Figure 8: proteomic analysis of CmRJ-Zj and BnRJ-Zj. (A) PCA analysis discriminated CmRJ-Zj from BnRJ-Zj. **(B)** Volcano plot showing $\log_2$FC against -$\log_{10}$ (*p* value) identified 7 up-regulated proteins and 3 down-regulated proteins in CmRJ-Zj vs. BnRJ-Zj.

3.9 Metabolomics of RJ

The small molecules present in CmRJ-Zj and BnRJ-Zj were identified and quantified by the untargeted metabolomic technique. Overlaid chromatograms of QC injection indicated good repeatability for the retention time, peak shape and intensity of the method (Figure S2). CmRJ-Zj and BnRJ-Zj could be clearly discriminated from each other as illustrated by principal component analysis (PCA) (Figure 9A-B) and orthogonal partial least squares discriminant analysis (OPLS-DA) (Figure 9C-D). A total of 631 differential compounds (468 up-regulated and 163 down-regulated in CmRJ-Zj vs. BnRJ-Zj) were identified with the criteria of variable importance in projection (VIP) > 1, *p* value < 0.05 (Student's *t*-test) and fold change >2 or < 0.5 (Figure 9E-F and Table S3). Heatmap

analysis also showed different chemical profile between CmRJ-Zj and BnRJ-Zj (Figure S3). According to KEGG analysis, the compounds present in CmRJ-Zj with significantly higher abundance were mainly involved in the pathway of oxidative phosphorylation (ko00190), nicotinate and nicotinamide metabolism (ko00760), longevity regulating pathway (ko04211), caffeine metabolism (ko00232), purine metabolism (ko00230), cGMP-PKG signalling pathway (ko04022), MAPK signalling pathway (ko04010), Rap1 signalling pathway (ko04015), chemokine signalling pathway (ko04062), platelet activation (ko04611), linoleic acid metabolism (ko00591), phenylalanine, tyrosine and tryptophan biosynthesis (ko00400), mineral absorption (ko04978), and riboflavin metabolism (ko00740) (Table S4).

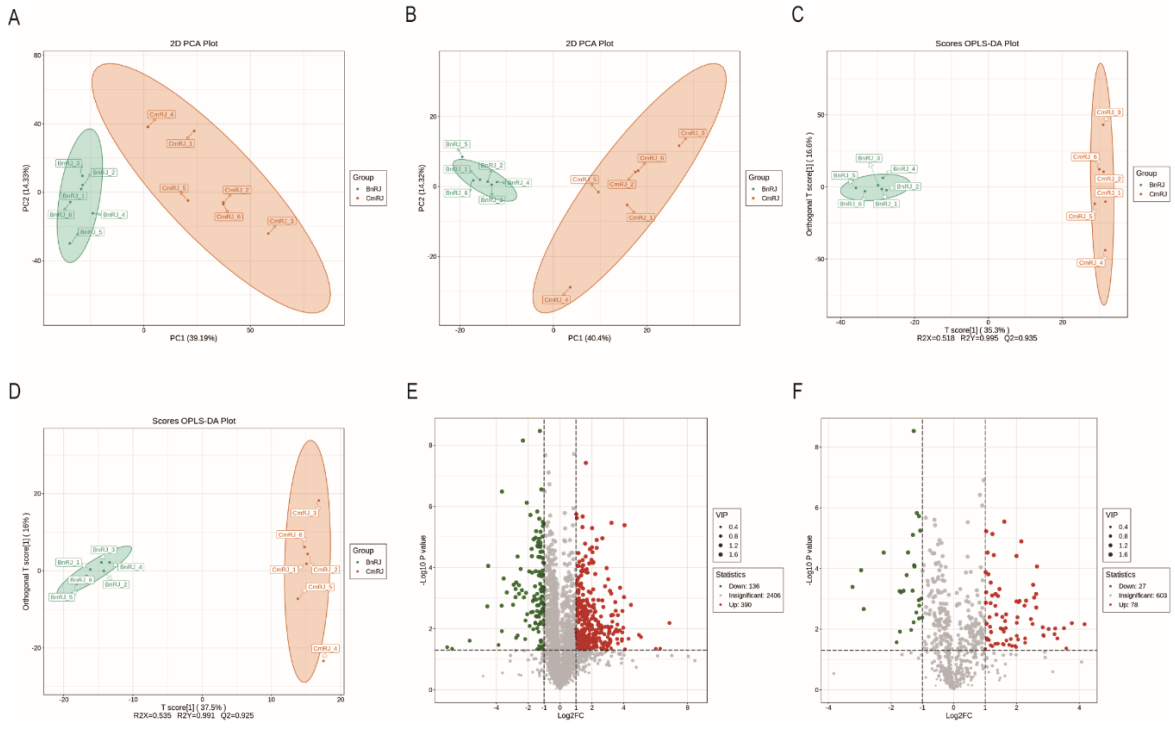

Figure 9: Untargeted metabolomic analysis of compounds in CmRJ-Zj and BnRJ-Zj. PCA plots showing discrimination between CmRJ-Zj and BnRJ-Zj in positive **(A)** and negative **(B)** ion modes. OPLS-DA plots indicating efficiency of the model and clear separation between CmRJ-Zj and BnRJ-Zj in positive **(C)** and negative **(D)** ion modes. Volcano plots showing $\log_2$FC against -$\log_{10}$ (*p* value) as well as VIPs identified 526 and 105 variables in positive **(E)** and negative **(F)** ion modes.

4 Discussion

In present-day society, non-healing wounds are an emerging global health issue, due to the high morbidity of some diseases such as diabetes, angiocardiopathy and obesity [1]. Despite advanced and modernised therapies, many kinds of chronic wounds are almost clinically untreatable, even leading to disability [2]. What is worse, is that there is no clinically effective and safe drug available for the treatment of these hard-to-heal wounds, increasing the burden on both patients and healthcare systems. Thus, wound-repairing facilitating agents are desiderata in clinical practice. RJ is a natural resource to exploit various pharmacologically-active components. One of the outstanding properties of RJ is its wound-healing effect, the use of which dates back to ancient times [13,15,16]. Regretfully, very few researchers have looked deeply into its mechanisms of action or tried to identify bioactive components to be developed into a drug, greatly restricting its application and the development of novel wound repair drugs. Based on relevant pre-clinical studies of RJ on animal models [13,15,16] and our previous study [17], here, the wound healing mechanisms of crude RJ derived from the blossom seasons of chestnut and rapeseed were further explored with a particular focus on the modulatory effects of CmRJ-Zj on some important signalling pathways and AQP3, and the ingredient profiles of these categories of RJ were also comprehensively investigated.

Keratinocytes are thought to be important cells throughout the wound healing process, whose proliferation and migration facilitate the re-epithelialization and eventual wound closure [34]. The *in vitro* tests on human epidermal keratinocytes (HaCaT) are considered reliable cell models for studying the effects of compounds on cutaneous wounds [35]. Hence, the proliferative and migratory activities of RJ from different floral sources/regions/sampling years, were first evaluated using the HaCaT cell line. As a result, RJ from the flowering season of chestnut, regardless of the harvesting time and regions, could directly boost the growth and mobility of HaCaT cells without obvious cytotoxicity at lower concentrations. On the other hand, rapeseed RJ was devoid of such efficacy and was toxic to the cells (Figure 1 and Figure 2), implying firstly, that crude chestnut RJ possessed potential wound healing-promoting activity, which was consistent with the effects previously observed in the *in vivo* wound model [17], and secondly that the pharmacological efficacies of RJ were

predominantly dependent on the floral origins. What is noteworthy, is that instead of displaying strict dose-dependent behaviour, chestnut RJ exhibited fluctuant proliferative effects on HaCaT cells at 48 h (Figure 1A-B), and it did not induce cell growth at 24 h (Figure S1), implying it might possess a relatively modest growth-promoting potency. The different tendency of CmRJ-Zj towards the growth and the mobility of keratinocytes (Figure 1A and Figure 2A) suggested that it might modulate cell proliferation and migration with different and intricate mechanisms. As expected, the effective concentration of CmRJ-Zj in the transwell assay was higher than that in the scratch wound assay (Figure 2A and C), since the potential cell proliferation would contribute to the motion of HaCaT cells in wounded monolayer to some extent.

In addition to presenting the effects of CmRJ-Zj on cellular proliferation and migration, we also investigated such signal transduction mechanisms probably implicated in the wound healing procedure as MAPK and Ca^{2+} pathways. ERK1/2 and p38, major groups of MAPKs, as well as extracellular/intracellular Ca^{2+}, were reported to play critical roles in wound healing by regulating cell mobility, apoptosis and proliferation [36–38]. Here, immunoblots demonstrated that exposed to CmRJ-Zj, the total protein level of p38 and ERK1/2 increased to some degrees within 6 h, and it was accompanied by their significant phosphorylation, resulting in the increased proportion of the phosphorylated forms (Figure 3A). The phosphorylation level of p38 was higher than that of ERK1/2, which was consistent with the stronger inhibition of SB203580 towards the CmRJ-Zj-mediated wound closure. The following decrease in the phosphorylation levels to the control level or below might be regulated by the negative feedback loop [39]. Such activation of p38 and ERK1/2, together with the suppressive effects of their canonical inhibitors on the CmRJ-Zj-induced wound closure, strongly suggested that CmRJ-Zj likely promoted HaCaT migration/growth via activating the upstream components of the MAPK signalling pathways [39]. By monitoring the variation of cytosolic free Ca^{2+}, CmRJ-Zj stimulated significant increase in the level of cellular Ca^{2+} in the presence of external Ca^{2+}, while this phenomenon was not observed in the Ca^{2+}-free medium or RJ-untreated cells (Figure 3B-C). In combination with the abolishment of CmRJ-Zj-induced cell confluence by

BAPTA-AM (Figure 3D), the data revealed that CmRJ-Zj could also accelerate wound closure by inducing Ca^{2+} influx and engaging in calcium signalling pathways.

As the maintenance of skin moisture is conducive to the natural healing of wounds [40–43], integral membrane proteins — aquaporins (AQPs) responsible for transporting water and/or glycerol were quantified. Among the 13 AQPs (AQP0-AQP12) identified in various mammalian cells, AQP1, AQP3 and AQP5 were found on the membrane of keratinocytes in epidermis, coordinating the migration and proliferation of keratinocytes, skin hydration, and sweat secretion [44–48]. Thus, this study inquired into the regulation of different RJ for the expression of AQPs. In qRT-PCR assays, only a single dose (15.63μg/ml) of CmRJ-Zj up-regulated the AQP3 expression at transcriptional level (Figure 4B). Interestingly, the protein level of AQP3 in HaCaT cells was inconsistent with the level of mRNA (Figure 4D), which might be attributed to the storage of AQP3 in keratinocytes or the space and time interval between transcription and translation. Thus, it would be meaningful to explore the relationship between the time and AQP3 expression in the future. Silencing of AQP3 and the resultant entire repression on the CmRJ-Zj-induced growth and migration of keratinocytes confirmed the critical role of AQP3 in wound healing mediated by CmRJ-Zj (Figure 5). As a matter of fact, it was reported that honey and propolis could promote wound healing by inducing H_2O_2 entry from extracellular milieu through AQP3 to increase intracellular reactive oxygen species (ROS), followed by increased extracellular Ca^{2+} influx and activation of Ca^{2+} signalling [29,35]. In addition, some studies reported that epidermal growth factor receptor (EGFR), PI3K, p38 and ERK signalling pathways were involved in AQP3 expression and cell migration [49,50]. Accordingly, the modulation of RJ on H_2O_2-AQP3-Ca^{2+} pathway, and the involvement of EGFR, PI3K, p38 and ERK signalling pathways in the RJ-mediated AQP3 expression and corresponding cell behaviour, would be worth carrying out.

Inflammation initiates within hours post-skin injury. It is characterized by the secretion of miscellaneous pro-inflammatory cytokines from macrophages to protect skin from infection and to pave the way for the subsequent proliferation phase [27,51]. Nonetheless, prolonged inflammation

usually leads to non-healing wounds [52]. Thus, managing inflammation is particularly important in dealing with chronic wounds. In the current study, the modulatory activities of RJ against inflammation were evaluated in LPS-induced macrophages. Both CmRJ-Zj and BnRJ-Zj could significantly inhibit the LPS-stimulated nitric oxide (NO) production (Figure 6C). NO is an important regulator derived from metabolism of L-arginine and is associated with inflammation, cell proliferation, migration and differentiation in skin healing [53]. The function of NO is biphasic, which induces cell growth and migration at lower dose (<50 nM) and arrests the response at higher dose (>100 nM) [54,55]. The LPS stimulation caused as much as 50 μM of NO secretion in RAW 264.7 cells in this study; thus, the inhibitory activities of both types of RJ were beneficial to relieve the inflammatory response and to enhance keratinocytes, fibroblasts, endothelial and vascular smooth muscle cells proliferation and migration, eventually facilitating wound healing [54,55]. In addition, both types of RJ enhanced the generation of TGF-β1 (Figure 6E). It is not only a kind of growth factor, promoting cell proliferation and facilitating re-epithelialization, but also a potent anti-inflammatory cytokine [56]; meanwhile, it can impair production of NO by increasing the activity of arginase to breakdown L-arginine and inhibiting the activity of NO synthase (iNOS) to reduce NO synthesis [54,57]. The positive effects of both kinds of RJ on the generation of TGF-β1 (Figure 6E) might contribute to the proliferation of cutaneous cells and also support their anti-inflammatory efficacy in the wound healing process. The opposing relationship between NO and TGF-β1 was also confirmed in the current study: that the production of NO was inversely correlated with the secretion of TGF-β1 (Figure 6C and E). Moreover, pro-inflammatory cytokines are critical elements in wound repair, regulating immune response as well as keratinocytes and fibroblasts growth [58]. TNF-α, a vital pro-inflammatory cytokine, promotes wound repair via inducing inflammation in the early stage, while it tends to be superabundant at abnormal wound sites, which is detrimental to wound healing [59]. Here, only BnRJ-Zj displayed weak inhibitory activity on LPS-induced TNF-α production in RAW 264.7 cells (Figure 6D), implying that it might also facilitate the healing of chronic wounds by suppressing the production of TNF-α at a high dose (1,000 μg/ml). Overall, with respect to anti-inflammation,

both chestnut and rapeseed RJ might have the potential to accelerate wound healing by weakening and shortening the inflammatory response, and boosting proliferation and migration of pivotal cells; therein, chestnut RJ possessed a more profound potency towards NO or TGF-β1 associated inflammation, while rapeseed RJ might also be effective towards the excessive production of TNF-α in non-healing wounds. Compared with our previous study, the similar effects of crude BnRJ-Zj on the regulation of NO, TGF-β1 and TNF-α, as well as on the cellular proliferation and migration, to its hydrophilic and lipophilic extracts, implied that the ineffectiveness of crude BnRJ-Zj on the *in vivo* wound model [17] might not be caused by antagonistic substances. In contrast, we speculated that BnRJ-Zj might exert potential wound healing-promoting activity in the inflammatory stage that obvious wound contraction could not be observed.

When measuring the cytotoxicity of RJ samples towards other skin cells, fibroblasts derived from human embryonic skin were selected. As shown in Figure 7A, CmRJ-Zj was safe because, at the concentrations that were effective to promote the proliferation, migration, activation of vital signalling pathways, and AQP3 expression of HaCaT cells (Figure 1-Figure 5), and to exhibit anti-inflammatory activity in RAW 264.7 cells (Figure 6), it did not reduce the viability of CCC-ESF-1 cells. It could also enhance the growth of fibroblasts at some concentrations. On the other hand, BnRJ-Zj did not have any proliferative effect on CCC-ESF-1 cells, and cytotoxicity was noted, which was similar to its effects on keratinocytes and macrophages. Additionally, in comparison with previous studies in which the RJ tested did not increase the cell viability of fibroblasts at lower concentrations (<5 μg/ml) and was toxic at higher concentrations (>10 μg/ml) [60,61], chestnut RJ might be a more effective and safer remedy for skin wounds than other types of RJ. In the future, the production of TGF-β1 and collagen in fibroblasts could be examined to explore the regulatory effects of chestnut RJ on tissue remodelling during wound healing [62].

Since RJ from different botanical origins exhibited significantly different efficacies on wound healing, it was necessary to further analyse the difference in the ingredient profiles, something which

has never previously been examined. According to the proteomic analysis, a total of 233 proteins were identified from CmRJ-Zj and BnRJ-Zj, 16 of which had been detected from RJ in previous studies [5,20,63–66] and 217 of which were new-found in this study (Table S5). Interestingly, among the major royal jelly proteins (MRJP1-MRJP9), MRJP8 was not detected in any RJ proteome (Table S5). Among the upregulated or uniquely expressed proteins in CmRJ-Zj (Table S1), chymotrypsin inhibitor, polyubiquitin-A isoform X2, glucose dehydrogenase isoform X2, ferritin heavy polypeptide-like 17, alpha-amylase precursor, venom serine carboxypeptidase isoform X1, transferrin 1 precursor might contribute to the potential wound-healing activity. Chymotrypsin inhibitor conduces to wound healing through maintaining the balance between the accumulation and degradation of extracellular matrix, inhibiting bacterial proteases together with anti-inflammation [67,68]. Glucose dehydrogenase isoform X2, ferritin heavy polypeptide-like 17, alpha-amylase precursor and transferrin 1 precursor can facilitate cellular proliferation or migration [69–73]. Polyubiquitin-A isoform X2 may not only stimulate cell growth, protein kinases and relevant signalling, but also possess antibacterial activity [74–76]. Venom serine carboxypeptidase isoform X1 may help clotting via its thrombin-like activity [77]. In contrast, the upregulation of esterase B1 present in BnRJ-Zj is related to cell apoptosis and is detrimental to wound healing [78]. These differentially expressed proteins, to some extent, explained the different modulatory effects of CmRJ-Zj and BnRJ-Zj on the cell behaviour and signalling observed in this study, and the *in vivo* wound healing observed in our previous study [17]. Among these functional proteins, except for alpha-amylase precursor, the other six were first identified from RJ, which illustrated the specific effects of CmRJ-Zj and BnRJ-Zj.

In regard to the metabolomic analysis, we found that among the significantly upregulated compounds in CmRJ-Zj ($log_2FC > 4$, Figure 9), N1,N1-dimethyl-4-[[4-(dimethylamino)phenyl](4-nitrophenyl)methyl]aniline (MW0008766), N1,N5,N10-tricaffeoyl spermidine (MW0154136), N6-isopentenyladenosine (MEDP1991), morphine-6-glucuronide (MW0000341) and benzenepropanoic acid (MW0006210) might be beneficial to the wound healing procedure, as they were associated with cell proliferation, anti-inflammation and/or abirritation [79–83]. In addition, as revealed by the KEGG

analysis, some of the highly enriched pathways with upregulated compounds in CmRJ-Zj were implicated in wound healing. For instance, platelet activation facilitates blood coagulation in the initial stage of injury [84]; oxidative phosphorylation, MAPK signalling pathway and Rap1 signalling pathway are related to the activation of p38 and ERK1/2 signalling pathways, as well as cell proliferation and migration[85,86]; chemokine signalling pathway and mineral absorption may explain the modulation of CmRJ-Zj in cellular Ca^{2+} level and subsequent cell migration [87,88]; nicotinate and nicotinamide metabolism, longevity regulating pathway, riboflavin metabolism, phenylalanine, tyrosine and tryptophan biosynthesis, and purine metabolism contribute to the synthesis of DNA and proteins, cell proliferation, anti-inflammation and antioxidation [89,90]. The presence of these compounds in CmRJ-Zj and the involvement of these signalling pathways also explained its remarkable effects on the wound healing procedure.

Overall, in combination with our previous study [17], the present study further elucidated that compared with rapeseed RJ, chestnut RJ possessed a dramatically more potent wound-healing activity which was associated with re-epithelialization, p38, ERK1/2, Ca^{2+} signalling pathways, AQP3 expression and anti-inflammation. It may be useful in the whole course for treating chronic wounds characterized by abnormal levels of cytokines and mediators, or weak proliferative and migratory capabilities of keratinocytes [91], opening up the application of chestnut RJ in wound healing and the development of relevant therapeutic agents. It will be worthwhile preparing different dosage forms and carrying out further study using animal models with various cutaneous injuries to analyse the histological and immunohistochemical changes in the wound healing process, thereby gaining further insight into the *in vivo* effects and mechanisms of chestnut RJ. In consideration of its *in vitro* cytotoxicity at higher doses in this study and the meaningful pharmacological doses [92], concentrations ranging from 7 to 200 μg/ml may be considered relatively safe to be tested for the future *in vivo* studies. Furthermore, the proteomic and metabolomic analysis revealed that chestnut RJ and rapeseed RJ possessed distinct molecular profile. It is the first time to comprehensively investigate the ingredients of RJ from different floral sources, providing clues to distinguish different types of RJ. Bioinformatic functional

analysis explained the corelation between molecular variability and bioactivities to some extent, which will help to find out the specific functional compounds or active domains. As the bioactivities of RJ are influenced by the botanical sources, it will be interesting to investigate the compositions and functions of the pollens from corresponding nectar plants to reveal the componential and functional relationships between pollens and RJ, which will greatly improve the application value of RJ.

5 Conclusions

In conclusion, the wound healing properties of RJ rely heavily on the botanical origins. Chestnut RJ presented the best performance in the wound healing procedure with cellular proliferative and migratory effects, modulation on vital signalling pathways, and anti-inflammatory functions. It may lead to a good treatment outcome for complex non-healing wounds. Thus, the current study confers the evidence for the rational use of different kinds of RJ as wound care agents and the development of therapeutic drugs for treating non-healing wounds. The proteomic and metabolomic results also improve our knowledge of the ingredient profiles of RJ from diverse floral sources for the better identification of RJ categories in the future.

Supplementary materials

Figure S1: Proliferative effect of CmRJ-Zj on HaCaT cells after treatment for 24 h. ***, $p < 0.001$, compared with control.

Figure S2: Overlaid chromatogram of QC injection in positive ion mode **(A)** and negative ion mode **(B)**.

Figure S3: Heatmap of differential compounds between CmRJ-Zj and BnRJ-Zj in positive ion mode (A) and negative ion mode (B). The levels of changed compounds are shown in rows with red representing increase and green representing decrease, and separated samples are shown in columns.

Table S1: Differentially expressed proteins in CmRJ-Zj and BnRJ-Zj.

Table S2: Compounds identified from CmRJ-Zj and BnRJ-Zj.

Table S3: Differential compounds in CmRJ-Zj and BnRJ-Zj.

Table S4: KEGG enrichment of the differential compounds in CmRJ-Zj and BnRJ-Zj

Table S5: Comparison of proteins identified from RJ in the present and previous studies.

Author Contributions

S.S. and Y.L. conceived and designed the experiments; M.Z., Y.L., T.L., L.W. and G.W. performed the experiments; Y.L., M.Z., T.L., T.C. and S.S. analysed the data; Y.L., S.S., T.C. and M.Z. wrote the paper. All authors read and approved the final manuscript.

Conflict of Interest

There are no conflicts to declare.

Acknowledgements

This work was supported by the grants from the Natural Science Foundation of Fujian Province (No. 2019J01408), the Outstanding Young Scientist Program of Fujian Agriculture and Forestry University (No. xjq201916), the National Natural Science Foundation of China (No. 31772684), and the Earmarked Fund for Modern Agro-industry Technology Research System (No. CARS-44-KXJ4).

References

1 C. K. Sen, G. M. Gordillo, S. Roy, R. Kirsner, L. Lambert, T. K. Hunt, F. Gottrup, G. C. Gurtner and M. T. Longaker, Human skin wounds: A major and snowballing threat to public health and the economy, *Wound Repair Regen.*, 2009, **17**, 763–771.

2 K. Järbrink, G. Ni, H. Sönnergren, A. Schmidtchen, C. Pang, R. Bajpai and J. Car, Prevalence and incidence of chronic wounds and related complications: A protocol for a systematic review, *Syst. Rev.*, 2016, **5**, 152.

3 C.-F. Cheng, D. Sahu, F. Tsen, Z. Zhao, J. Fan, R. Kim, X. Wang, K. O'Brien, Y. Li, Y. Kuang, M. Chen, D. T. Woodley and W. Li, A fragment of secreted Hsp90α carries properties that enable it to accelerate effectively both acute and diabetic wound healing in mice, *J. Clin. Invest.*, 2011, **121**, 4348–4361.

4 M. Hellner, D. Winter, R. von Georgi and K. Münstedt, Apitherapy: Usage and experience in german beekeepers, *Evid. Based Complement. Alternat. Med.*, 2008, **5**, 475–479.

5 F. Yu, F. Mao and L. Jianke, Royal jelly proteome comparison between A. mellifera ligustica and A. cerana cerana, *J. Proteome Res.*, 2010, **9**, 2207–2215.

6 A. M. Ali and H. Kunugi, Royal jelly as an intelligent anti-aging agent-A focus on cognitive aging and Alzheimer's disease: A review, *Antioxidants*, 2020, **9**, 937.

7 K. Bílikova, S.-C. Huang, I.-P. Lin, J. Šimuth and C.-C. Peng, Structure and antimicrobial activity relationship of royalisin, An antimicrobial peptide from royal jelly of Apis mellifera, *Peptides*, 2015, **68**, 190–196.

8 T. Karaca, N. Şimşek, S. Uslu, Y. Kalkan, I. Can, A. Kara and M. Yörük, The effect of royal jelly on CD3(+), CD5(+), CD45(+) T-cell and CD68(+) cell distribution in the colon of rats with acetic acid-induced colitis, *Allergol. Immunopathol. (Madr)*, 2012, **40**, 357–361.

9 Y. Kimura, Antitumor and antimetastatic actions of various natural products, *Stud. Nat. Prod. Chem.*, 2008, **34**, 35–76.

10 D. Mihajlovic, D. Vucevic, I. Chinou and M. Colic, Royal jelly fatty acids modulate proliferation and cytokine production by human peripheral blood mononuclear cells, *Eur. Food Res. Technol.*, 2014, **238**, 881–887.

11 S. Pourmoradian, R. Mahdavi, M. Mobasseri, E. Faramarzi and M. Mobasseri, Effects of royal jelly supplementation on glycemic control and oxidative stress factors in type 2 diabetic female: A randomized clinical trial, *Chin. J. Integr. Med.*, 2014, **20**, 347–352.

12 S. Ahmad, M. G. Campos, F. Fratini, S. Z. Altaye and J. Li, New insights into the biological and pharmaceutical properties of royal jelly, *Int. J. Mol. Sci.*, 2020, **21**, 382.

13 M. Abdelatif, M. Yakoot and M. Etmaan, Safety and efficacy of a new honey ointment on diabetic foot ulcers: A prospective pilot study, *J. Wound Care*, 2008, **17**, 108–110.

14 M. Bucekova, M. Sojka, I. Valachova, S. Martinotti, E. Ranzato, Z. Szep, V. Majtan, J. Klaudiny and J. Majtan, Bee-derived antibacterial peptide, defensin-1, promotes wound re-epithelialisation in vitro and in vivo, *Sci. Rep.*, 2017, **7**, 7340.

15 M. H. El-Gayar, K. M. Aboshanab, M. M. Aboulwafa and N. A. Hassouna, Antivirulence and wound healing effects of royal jelly and garlic extract for the control of MRSA skin infections, *Wound Med.*, 2016, **13**, 18–27.

16 F. K. Temamogullari, Comparison of the royal jelly and povidone iodine on wound healing in rabbits, *J. Anim. Vet. Adv.*, 2007, **6**, 203–205.

17 Y. Lin, M. Zhang, L. Wang, T. Lin, G. Wang, J. Peng and S. Su, The in vitro and in vivo wound-healing effects of royal jelly derived from Apis mellifera L. during blossom seasons of Castanea mollissima Bl. and Brassica napus L. in South China exhibited distinct patterns, *BMC Complement. Med. Ther.*, 2020, **20**, 357.

18 A. Gismondi, E. Trionfera, L. Canuti, G. Di Marco and A. Canini, Royal jelly lipophilic fraction induces antiproliferative effects on SH-SY5Y human neuroblastoma cells, *Oncol. Rep.*, 2017, **38**, 1833–1844.

19 Y. Zhao, Z. Li, W. Tian, X. Fang, S. Su and W. Peng, Differential volatile organic compounds in royal jelly associated with different nectar plants, *J. Integr. Agric.*, 2016, **15**, 1157–1165.

20 J. Li, T. Wang, Z. Zhang and Y. Pan, Proteomic analysis of royal jelly from three strains of western honeybees (Apis mellifera), *J. Agric. Food Chem.*, 2007, **55**, 8411–8422.

21 D. Qi, C. Ma, W. Wang, L. Zhang and J. Li, Gas chromatography-mass spectrometry analysis as a tool to reveal differences between the volatile compound profile of royal jelly produced from Tea and Pagoda trees, *Food Anal. Methods*, 2021, **14**, 616-630.

22 M. C. Garcia, M. S. Finola and J. M. Marioli, Bioassay directed identification of royal jelly's active compounds against the growth of bacteria capable of infecting cutaneous wounds, *Adv. Microbiol.*, 2013, **03**, 138–144.

23 M. C. Garc á, M. S. Finola and J. M. Marioli, Antibacterial activity of royal jelly against bacteria capable of infecting cutaneous wounds, *J. ApiProd. ApiMed. Sci.*, 2010, **2**, 93–99.

24 Y. Lin, Q. Shao, M. Zhang, C. Lu, J. Fleming and S. Su, Royal jelly-derived proteins enhance proliferation and migration of human epidermal keratinocytes in an in vitro scratch wound model, *BMC Complement. Altern. Med.*, 2019, **19**, 175.

25 H. Song, Y. Zhang, N. Liu, D. Zhang, C. Wan, S. Zhao, Y. Kong and L. Yuan, Let-7b inhibits the malignant behavior of glioma cells and glioma stem-like cells via downregulation of E2F2, *J. Physiol. Biochem.*, 2016, **72**, 733–744.

26 S. Hao, S. Li, J. Wang, Y. Yan, X. Ai, J. Zhang, Y. Ren, T. Wu, L. Liu and C. Wang, Phycocyanin exerts anti-proliferative effects through down-regulating TIRAP/NF-κB activity in human non-small cell lung cancer cells, *Cells*, 2019, **8**, 588.

27 B. K. Sun, Z. Siprashvili and P. A. Khavari, Advances in skin grafting and treatment of cutaneous wounds, *Science*, 2014, **346**, 941–945.

28 M. Hara-Chikuma and A. S. Verkman, Roles of aquaporin-3 in the epidermis, *J. Invest. Dermatol.*, 2008, **128**, 2145–2151.

29 S. Martinotti, U. Laforenza, M. Patrone, F. Moccia and E. Ranzato, Honey-mediated wound healing: H_2O_2 entry through AQP3 determines extracellular Ca^{2+} influx, *Int. J. Mol. Sci.*, 2019, **20**, 764.

30 K. Nakahigashi, K. Kabashima, A. Ikoma, A. S. Verkman, Y. Miyachi and M. Hara-Chikuma, Upregulation of Aquaporin-3 is involved in keratinocyte proliferation and epidermal hyperplasia, *J. Invest. Dermatol.*, 2011, **131**, 865–873.

31 A. Kure, K. Nakagawa, M. Kondo, S. Kato, F. Kimura, A. Watanabe, N. Shoji, S. Hatanaka, T. Tsushida and T. Miyazawa, Metabolic fate of luteolin in rats: Its relationship to anti-inflammatory effect, *J. Agric. Food Chem.*, 2016, **64**, 4246–4254.

32 Y. Wu, F. Han, S. Luan, R. Ai, P. Zhang, H. Li and L. Chen, Triterpenoids from ganoderma lucidum and their potential anti-inflammatory effects, *J. Agric. Food Chem.*, 2019, **67**, 5147–5158.

33 J. Ma, T. Chen, S. Wu, C. Yang, M. Bai, K. Shu, K. Li, G. Zhang, Z. Jin, F. He, H. Hermjakob and Y. Zhu, IProX: An integrated proteome resource, *Nucleic Acids Res.*, 2019, **47**, 1211–1217.

34 E. A. Gantwerker and D. B. Hom, Skin: Histology and physiology of wound healing, *Facial Plast. Surg. Clin. North Am.*, 2011, **19**, 441–453.

35 S. Martinotti, G. Pellavio, U. Laforenza and E. Ranzato, Propolis induces AQP3 expression: A possible way of action in wound healing, *Molecules*, 2019, **24**, 1544.

36 H. Cheng, S. Wei, L. Wei and A. Verkhratsky, Calcium signaling in physiology and pathophysiology, *Acta Pharmacol. Sin.*, 2006, **27**, 767–772.

37 A. B. G. Lansdown, Calcium: Apotential central regulator in wound healing in the skin, *Wound Repair Regen.*, 2002, **10**, 271–285.

38 R. Seger and E. G. Krebs, The MAPK signaling cascade, *FASEB J.*, 1995, **9**, 726–735.

39 A. Glady, A. Vandebroek and M. Yasui, Human keratinocyte-derived extracellular vesicles activate the MAPKinase pathway and promote cell migration and proliferation in vitro, *Inflamm. Regen.*, 2021, **41**, 4.

40 J. S. Boateng, K. H. Matthews, H. N. E. Stevens and G. M. Eccleston, Wound healing dressings and drug delivery systems: A review, *J. Pharm. Sci.*, 2008, **97**, 2892–2923.

41 X. Liu, T. Lin, J. Fang, G. Yao, H. Zhao, M. Dodson and X. Wang, In vivo wound healing and antibacterial performances of electrospun nanofibre membranes, *J. Biomed. Mater. Res. A*, 2010, **94**, 499–508.

42 K. Velding, S.-A. Klis, K. M. Abass, W. Tuah, Y. Stienstra and T. van der Werf, Wound care in Buruli ulcer disease in Ghana and Benin, *Am. J. Trop. Med. Hyg.*, 2014, **91**, 313–318.

43 A. S. Verkman, M. Hara-Chikuma and M. C. Papadopoulos, Aquaporins-new players in cancer biology, *J. Mol. Med.*, 2008, **86**, 523–529.

44 T. Ma, M. Hara, R. Sougrat, J.-M. Verbavatz and A. S. Verkman, Impaired stratum corneum hydration in mice lacking epidermal water channel aquaporin-3, *J. Biol. Chem.*, 2002, **277**, 17147–17153.

45 L. N. Nejsum, T.-H. Kwon, U. B. Jensen, O. Fumagalli, J. Frøkiaer, C. M. Krane, A. G. Menon, L. S. King, P. C. Agre and S. Nielsen, Functional requirement of aquaporin-5 in plasma membranes of sweat glands, *Proc. Natl. Acad. Sci. U.S.A.*, 2002, **99**, 511–516.

46 M. C. Papadopoulos, S. Saadoun and A. S. Verkman, Aquaporins and cell migration, *Pflugers. Arch.*, 2008, **456**, 693–700.

47 R. Patel, L. Kevin Heard, X. Chen and W. B. Bollag, Aquaporins in the skin, *Adv. Exp. Med. Biol.*, 2017, **969**, 173–191.

48 S. Y. Shin, D. H. Lee, H.-N. Gil, B. S. Kim, J.-S. Choe, J.-B. Kim, Y. H. Lee and Y. Lim, Agerarin, identified from Ageratum houstonianum, stimulates circadian CLOCK-mediated aquaporin-3 gene expression in HaCaT keratinocytes, *Sci. Rep.*, 2017, **7**, 11175.

49 H.-M. Ryu, E.-J. Oh, S.-H. Park, C.-D. Kim, J.-Y. Choi, J.-H. Cho, I.-S. Kim, T.-H. Kwon, H.-Y. Chung, M. Yoo and Y.-L. Kim, Aquaporin 3 expression is up-regulated by TGF-β1 in rat peritoneal mesothelial cells and plays a role in wound healing, *Am. J. Pathol.*, 2012, **181**, 2047–2057.

50 C. Cao, Y. Sun, S. Healey, Z. Bi, G. Hu, S. Wan, N. Kouttab, W. Chu and Y. Wan, EGFR-mediated expression of aquaporin-3 is involved in human skin fibroblast migration, *Biochem. J.*, 2006, **400**, 225–234.

51 A. S. Verkman, Aquaporins at a glance, *J. Cell Sci.*, 2011, **124**, 2107–2112.

52 R. J. Snyder, J. Lantis, R. S. Kirsner, V. Shah, M. Molyneaux and M. J. Carter, Macrophages: A review of their role in wound healing and their therapeutic use, *Wound Repair Regen.*, 2016, **24**, 613–629.

53 P. Abaffy, S. Tomankova, R. Naraine, M. Kubista and R. Sindelka, The role of nitric oxide during embryonic wound healing, *BMC Genomics*, 2019, **20**, 815.

54 S. Frank, H. Kämpfer, C. Wetzler and J. Pfeilschifter, Nitric oxide drives skin repair: Novel functions of an established mediator, *Kidney Int.*, 2002, **61**, 882–888.

55 J. S. Isenberg, W. A. Frazier and D. D. Roberts, Thrombospondins: From structure to therapeutics: Thrombospondin-1: A physiological regulator of nitric oxide signaling, *Cell. Mol. Life Sci.*, 2008, **65**, 728–742.

56 C. Dai, X. Wen, W. He and Y. Liu, Inhibition of proinflammatory RANTES expression by TGF-beta1 is mediated by glycogen synthase kinase-3beta-dependent beta-catenin signaling, *J. Biol. Chem.*, 2011, **286**, 7052–7059.

57 M. B. Witte and A. Barbul, Role of nitric oxide in wound repair, *Am. J. Surg.*, 2002, **183**, 406–412.

58 S. Werner and R. Grose, Regulation of wound healing by growth factors and cytokines, *Physiol. Rev.*, 2003, **83**, 835–870.

59 J. Wedler, T. Daubitz, G. Schlotterbeck and V. Butterweck, In vitro anti-inflammatory and wound-healing potential of a phyllostachys edulis leaf extract – Identification of isoorientin as an active compound, *Planta Med.*, 2014, **80**, 1678–1684.

60 J. Kim, Y. Kim, H. Yun, H. Park, S. Y. Kim, K.-G. Lee, S.-M. Han and Y. Cho, Royal jelly enhances migration of human dermal fibroblasts and alters the levels of cholesterol and sphinganine in an in vitro wound healing model, *Nutr. Res. Pract.*, 2010, **4**, 362–368.

61 H. M. Park, E. Hwang, K. G. Lee, S.-M. Han, Y. Cho and S. Y. Kim, Royal jelly protects against ultraviolet B-induced photoaging in human skin fibroblasts via enhancing collagen production, *J. Med. Food*, 2011, **14**, 899–906.

62 K.-M. Satomi, O. Iwao, U. Shimpei, I. Kanso, I. Masao and K. Masashi, Identification of a collagen production-promoting factor from an extract of royal jelly and its possible mechanism, *Biosci. Biotechnol. Biochem.*, 2004, **68**, 767–73.

63 F. Toshiyuki, K.-H. Hiroko, A.-K. Hiroko, K. Takekazu, O. Masaaki and K. Takeo, Proteomic analysis of the royal jelly and characterization of the functions of its derivation glands in the honeybee, *J. Proteome Res.*, 2013, **12**, 404–411.

64 T. Furusawa, R. Rakwal, H. W. Nam, J. Shibato, G. K. Agrawal, Y. S. Kim, Y. Ogawa, Y. Yoshida, Y. Kouzuma, Y. Masuo and M. Yonekura, Comprehensive royal jelly (RJ) proteomics using one- and two-dimensional proteomics platforms reveals novel RJ proteins and potential phospho/glycoproteins, *J. Proteome Res.*, 2008, **7**, 3194–3229.

65 B. Han, C. Li, L. Zhang, Y. Fang, M. Feng and J. Li, Novel royal jelly proteins identified by gel-based and gel-free proteomics, *J. Agric. Food Chem.*, 2011, **59**, 10346–10355.

66 S. Schönleben, A. Sickmann, M. J. Mueller and J. Reinders, Proteome analysis of Apis mellifera royal jelly, *Anal. Bioanal. Chem.*, 2007, **389**, 1087–1093.

67 M. S. Lantz, Are bacterial proteases important virulence factors?, *J. Periodontal Res.*, 1997, **32**, 126–132.

68 S. M. McCarty and S. L. Percival, Proteases and delayed wound healing., *Adv. Wound Care (New Rochelle)*, 2013, **2**, 438–447.

69 M. F. Carlevaro, A. Albini, D. Ribatti, C. Gentili, R. Benelli, S. Cermelli, R. Cancedda and F. D. Cancedda, Transferrin promotes endothelial cell migration and invasion: Implication in cartilage neovascularization, *J. Cell Biol.*, 1997, **136**, 1375–1384.

70 I. Graziadei, C. M. Kähler, C. J. Wiedermann and W. Vogel, The acute-phase protein alpha 1-antitrypsin inhibits transferrin-receptor binding and proliferation of human skin fibroblasts, *Biochim. Biophys. Acta*, 1998, **1401**, 170–176.

71 K. Date, T. Yamazaki, Y. Toyoda, K. Hoshi and H. Ogawa, α-Amylase expressed in human small intestinal epithelial cells is essential for cell proliferation and differentiation, *J. Cell Biochem.*, 2020, **121**, 1238–1249.

72 Y. Zhang, Y. Li, J. Wang and P. Lei, Long non-coding RNA ferritin heavy polypeptide 1 pseudogene 3 controls glioma cell proliferation and apoptosis via regulation of the microRNA-224-5p/tumor protein D52 axis, *Mol. Med. Rep.*, 2018, **18**, 4239–4246.

73 B. M. Zimmer, J. J. Barycki and M. A. Simpson, Integration of sugar metabolism and proteoglycan synthesis by UDP-glucose dehydrogenase, *J. Histochem. Cytochem.*, 2021, **69**, 13–23.

74 C.-W. Park, J.-S. Bae and K.-Y. Ryu, Simultaneous disruption of both polyubiquitin genes affects proteasome function and decreases cellular proliferation, *Cell Biochem. Biophys.*, 2020, **78**, 321–329.

75 J.-K. Seo, M. J. Lee, H.-J. Go, G. D. Kim, H. D. Jeong, B.-H. Nam and N. G. Park, Purification and antimicrobial function of ubiquitin isolated from the gill of Pacific oyster, Crassostrea gigas, *Mol. Immunol.*, 2013, **53**, 88–98.

76 D. Komander, The emerging complexity of protein ubiquitination, *Biochem. Soc. Trans.*, 2009, **37**, 937–953.

77 D. Mel éndez-Mart ínez, L. F. Plenge-Tellechea, A. Gatica-Colima, M. S. Cruz-P érez, J. M. Aguilar-Y áñez and C. Licona-Cassani, Functional mining of the Crotalus Spp. venom protease repertoire reveals potential for chronic wound therapeutics, *Molecules*, 2020, **25**, 3401.

78 J. A. Malla, V. K. Sharma, M. Lahiri and P. Talukdar, Esterase-activatable synthetic M^+/Cl^- channel induces apoptosis and disrupts autophagy in cancer cells, *Chemistry*, 2020, **26**, 11946–11949.

79 R. K. Verma, M. Pandey, M. D. Indoria, R. Singh and S. Suthar, Phytochemical investigation and pharmacological evaluation of leaves of Ziziphus mauritiana for wound healing activity in albino rats, *TJPLS J.*, 2018, **5**, 8-18.

80 E. L. A.Dorp, A. Morariu and A. Dahan, Morphine-6-glucuronide: Potency and safety compared with morphine, *Expert Opin. Pharmacother.*, 2008, **9**, 1955–1961.

81 A. Santoro, E. Ciaglia, V. Nicolin, A. Pescatore, L. Prota, M. Capunzo, M. V. Ursini, S. L. Nori and M. Bifulco, The isoprenoid end product N6-isopentenyladenosine reduces inflammatory response through the inhibition of the NFκB and STAT3 pathways in cystic fibrosis cells, *Inflamm. Res.*, 2018, **67**, 315–326.

82 M. Hasan, S. Genovese, S. Fiorito, F. Epifano and P. A. Witt-Enderby, Oxyprenylated phenylpropanoids bind to MT1 melatonin receptors and inhibit breast cancer cell proliferation and migration, *J. Nat. Prod.*, 2017, **80**, 3324–3329.

83 J. Wang, G. Wang, H. Ma and M. F. Khan, Enhanced expression of cyclins and cyclin-dependent kinases in aniline-induced cell proliferation in rat spleen, *Toxicol. Appl. Pharmacol*, 2011, **250**, 213–220.

84 J. W. M. Heemskerk, E. M. Bevers and T. Lindhout, Platelet activation and blood coagulation, *Thromb. Haemost.*, 2002, **88**, 186–193.

85 Q. Li, Y. Teng, J. Wang, M. Yu, Y. Li and H. Zheng, Rap1 promotes proliferation and migration of vascular smooth muscle cell via the ERK pathway, *Pathol. Res. Pract.*, 2018, **214**, 1045–1050.

86 W.-S. Choi, D.-S. Eom, B. S. Han, W. K. Kim, B. H. Han, E.-J. Choi, T. H. Oh, G. J. Markelonis, J. W. Cho and Y. J. Oh, Phosphorylation of p38 MAPK induced by oxidative stress is linked to activation of both caspase-8- and -9-mediated apoptotic pathways in dopaminergic neurons, *J. Biol. Chem.*, 2004, **279**, 20451–20460.

87 C. M. Weaver and M. Peacock, Calcium, *Adv. Nutr.*, 2019, **10**, 546–548.

88 M. O'Hayre, C. L. Salanga, P. C. Dorrestein and T. M. Handel, Phosphoproteomic analysis of chemokine signaling networks, *Methods Enzymol.*, 2009, **460**, 331–346.

89 E. Nakano, S. Mushtaq, P. R. Heath, E.-S. Lee, J. P. Bury, S. A. Riley, H. J. Powers and B. M. Corfe, Riboflavin depletion impairs cell proliferation in adult human duodenum: Identification of potential effectors, *Dig. Dis. Sci.*, 2011, **56**, 1007–1019.

90 S. J. Yang, J. M. Choi, L. Kim, S. E. Park, E. J. Rhee, W. Y. Lee, K. W. Oh, S. W. Park and C.-Y. Park, Nicotinamide improves glucose metabolism and affects the hepatic NAD-sirtuin pathway in a rodent model of obesity and type 2 diabetes, *J. Nutr. Biochem.*, 2014, **25**, 66–72.

91 P. Governa, G. Carullo, M. Biagi, V. Rago and F. Aiello, Evaluation of the In vitro wound-healing activity of Calabrian honeys, *Antioxidants*, 2019, **8**, 36.

92 M. Heinrich, G. Appendino, T. Efferth, R. Fürst, A. A. Izzo, O. Kayser, J. M. Pezzuto and A. Viljoen, Best practice in research – Overcoming common challenges in phytopharmacological research, *J. Ethnopharmacol.*, 2020, **246**, 112230.